

Crystal Structure of a Conformation-selective Casein Kinase-1 Inhibitor*

Received for publication, March 2, 2000, and in revised form, April 2, 2000
Published, JBC Papers in Press, April 3, 2000, DOI 10.1074/jbc.M001713200

Neda Mashhoon[‡], Anthony J. DeMaggio[§], Valentina Tereshko^{||}, Stephen C. Bergmeier^{||},
Martin Egli^{||}, Merl F. Hoekstra[§], and Jeff Kuret^{‡**}

From the [‡]Center for Biotechnology, Ohio State University College of Medicine, Columbus, Ohio 43210, [§]ICOS Corporation, Bothell, Washington 98021, the ^{||}Department of Molecular Pharmacology and Biological Chemistry, Northwestern University Medical School, Chicago, Illinois 60611, and the ^{||}Division of Medicinal Chemistry, Ohio State University College of Pharmacy, Columbus, Ohio 43210

Members of the casein kinase-1 family of protein kinases play an essential role in cell regulation and disease pathogenesis. Unlike most protein kinases, they appear to function as constitutively active enzymes. As a result, selective pharmacological inhibitors can play an important role in dissection of casein kinase-1-dependent processes. To address this need, new small molecule inhibitors of casein kinase-1 acting through ATP-competitive and ATP-noncompetitive mechanisms were isolated on the basis of *in vitro* screening. Here we report the crystal structure of 3-[(2,4,6-trimethoxyphenyl)methylidene]indolin-2-one (IC261), an ATP-competitive inhibitor with differential activity among casein kinase-1 isoforms, in complex with the catalytic domain of fission yeast casein kinase-1 refined to a crystallographic *R*-factor of 22.4% at 2.8 Å resolution. The structure reveals that IC261 stabilizes casein kinase-1 in a conformation midway between nucleotide substrate liganded and nonliganded conformations. We propose that adoption of this conformation by casein kinase-1 family members stabilizes a delocalized network of side chain interactions and results in a decreased dissociation rate of inhibitor.

Mammalian casein kinase-1 (CK1)¹ is a protein kinase family consisting of multiple isoforms encoded by distinct genes (Cki α , β , γ 1, γ 2, γ 3, δ , ϵ). Family members contain a highly conserved ~290-residue N-terminal catalytic domain coupled to a variable C-terminal region that ranges in size from 40 to 180 amino acids (1). The C-terminal region serves to promote

differential subcellular localization of individual isoforms (2, 3) and to modulate enzyme activity (4).

Although their biological function is not understood in molecular detail, recent evidence suggests that CK1 isoforms play a role in regulation of DNA repair (5, 6), cellular morphology (7), circadian rhythm (8), and stabilization of cellular proteins such as β -catenin (9, 10) and membrane-bound transporters (11) against degradation. These phenotypes, combined with observations that different CK1 homologs are essential for intracellular trafficking in different cellular compartments (12–14), suggest that CK1 isozymes directly influence protein turnover and other transport-dependent cellular processes such as autophagy and secretion.

In addition to their roles in normal cell biology, at least one CK1 isoform, Cki δ , has been implicated in the pathogenesis of Alzheimer's disease (15, 16). Its colocalization with tau-containing neuronal inclusions (neurofibrillary tangles and Pick bodies), but not tau negative inclusions (Lewy bodies, Hirano bodies, and Marinesco bodies), is consistent with this isoform participating in the pathological hyperphosphorylation of tau protein in a range of neurodegenerative diseases (17). Indeed, the highly elevated levels of Cki δ found in Alzheimer's disease and its association with hallmark lesions of neurodegeneration suggest it is part of a final pathway of degeneration common to Alzheimer's disease, progressive supranuclear palsy, and amyotrophic lateral sclerosis (17).

In light of these findings, selective and potent inhibitors of CK1 are needed to help resolve the role of CK1 homologs in cell regulation and may have utility in the treatment of neurodegenerative disease. Two selective CK1 inhibitors have been reported. The first is *N*-(2-aminoethyl)-5-chloroisoquinoline-8-sulfonamide, also known as CKI7 (18). It is one of a large family of naphthalene and isoquinoline sulfonamide derivatives that compete with nucleotide substrate binding and that differ in potency and selectivity among protein kinases (reviewed in Ref. 19). As a result, individual isoquinoline sulfonamides have emerged as popular pharmacological tools for inhibiting CK1 activity in broken cell preparations. Nonetheless, the presence of a primary amine moiety on CKI7 renders it charged at physiological pH and of poor utility in intact cells and tissues. Other selective CK1 inhibitors are ribofuranosyl-benzimidazoles (20). Some of these are potent inhibitors of both CK1 and casein kinase-2 and also inhibit RNA polymerase. Relative selectivity among CK1 isoforms has not been shown with either CKI7 or the ribofuranosyl-benzimidazoles.

Using a C-terminal truncation mutant (Cki1 Δ 298) of Cki1 (one of five CK1 isoforms in fission yeast), we recently determined the structural basis of CK1 substrate selectivity and regulation using x-ray crystallography (21, 22). Subsequently,

* This work was supported in part by National Institutes of Health Grant GM56292 (to J. K.). The costs of publication of this article were defrayed in part by the payment of page charges. This article must therefore be hereby marked "advertisement" in accordance with 18 U.S.C. Section 1734 solely to indicate this fact.

The atomic coordinates and structure factors (code 1EH4) have been deposited in the Protein Data Bank, Research Collaboratory for Structural Bioinformatics, Rutgers University, New Brunswick, NJ (<http://www.rcsb.org/>).

** To whom correspondence should be addressed: Ohio State University Medical School, Dept. of Medical Biochemistry, 1060 Carmack Rd., Columbus, OH 43210. Tel.: 614-688-5899; Fax: 614-292-5379; E-mail: kuret.3@osu.edu.

¹ The abbreviations used are: CK1, casein kinase-1; AMP-PCP, β , γ -methyleneadenosine 5'-triphosphate; CKI7, *N*-(2-aminoethyl)-5-chloroisoquinoline-8-sulfonamide; FGFR, fibroblast growth factor receptor; IC261, 3-[(2,4,6-trimethoxyphenyl)methylidene]indolin-2-one; SU4984, 3-[4-(1-formylpiperazin-4-yl)benzylidene]indolin-2-one; SU5402, 3-[(3-(2-carboxyethyl)-4-methylpyrrol-2-yl)methylidene]indolin-2-one; PKA, cAMP-dependent protein kinase catalytic subunit; MOPS, 4-morpholinepropanesulfonic acid.

the structure of Cki1Δ298 in complex with CKI7 was solved to clarify how the inhibitory selectivity of CKI7 and other isoquinoline sulfonamide inhibitors was achieved (23). Here we report the use of high throughput screening of a library of small molecules to obtain a novel CK1-selective inhibitor, IC261, and its structure in complex with Cki1Δ298 determined by x-ray crystallography. The results show that IC261 is an ATP-competitive inhibitor that stabilizes Cki1Δ298 in an inactive conformation. Because of its affinity and neutral charge, IC261 can serve as a new generation of CK1 inhibitor potentially active in intact cells.

EXPERIMENTAL PROCEDURES

Materials—CK1 isoforms from *Schizosaccharomyces pombe* (Cki1Δ298) and human (Ckiα₁, Ckiδ, and Ckiε) were prepared as described previously (15, 16, 21). Bovine heart PKA was prepared as described previously (24) and kindly supplied by Dr. John Scott (Oregon Health Sciences University), *Pisaster ochraceus* cyclin-dependent protein kinase p34^{cdc2}, bovine thymus p55^{lyn}, and their substrate peptides were purchased from Upstate Biotechnology, Inc. Aluminum-backed silica gel (0.25-mm) plates were purchased from EM Separation Technologies. Deuterated solvents were purchased from Aldrich. A small molecule library suitable for random screening was assembled from commercial sources and in-house chemistry resources at ICOS Corp. The library included IC261. Coordinates for models of Cki1Δ298 in complex with MgATP (1CSN) and CKI7 (2CSN), for truncated mammalian Ckiδ apoenzyme (1CKJ), and for FGFR kinase in complex with inhibitors SU5402 (1FGI) and SU4984 (1AGW) were obtained from the Protein Data Bank, whereas FGFR kinase in complex with AMP-PCP (25) was provided by Dr. S. R. Hubbard (New York University, New York, NY).

Phosphotransferase Assays—Casein kinase activity was assayed at 37 °C as described previously (2). The standard reaction (40 μl) contained 25 mM 2-(*N*-morpholino)ethanesulfonic acid, pH 6.5, 50 mM NaCl, 15 mM MgCl₂, 2 mg/ml casein, 2 mM EGTA, 100 μM [γ-³²P]ATP (100–400 cpm/pmol). Initial velocity measurements were carried out in duplicate with ATP as the varied substrate. Kinetic constants and their standard errors were calculated as described in Ref. 26. For assay of inhibitor potency (IC₅₀), [γ-³²P]ATP was held constant (10 μM), whereas IC261 concentration was varied (0.1, 0.3, 1, 3, and 10 μM). To assess kinetic mechanism, inhibitors were held constant (IC261, 20 μM; IC3608, 100 μM), whereas [γ-³²P]ATP was varied as above. For screening small molecule libraries, CK1 isoforms (Ckiα₁, δ, and ε) were assayed as above except that casein was used at 10 mg/ml, [γ-³²P]ATP was held constant at 2 μM or 1 mM.

PKA, p34^{cdc2}, and p55^{lyn} were assayed using the phosphocellulose method (27) and synthetic peptide substrates Kemptide (33 μM in 5 mM HEPES, pH 7.5, 15 mM MgCl₂, 1 mM EGTA, 1 mM dithiothreitol; Ref. 28), PKTPKKAKKL (20 μM in 20 mM Tris-HCl, pH 7.5, 10 mM MgCl₂, 1 mM dithiothreitol; Ref. 29), and KVEKIGEGTYGVVYK (20 μM in 20 mM HEPES, pH 7.2, 10 mM MnCl₂, 1 mM dithiothreitol; Ref. 30), respectively. Assays contained 10 μM [γ-³²P]ATP and variable concentrations of inhibitors. The resultant data were fit to the following relationship.

$$A = A_0 + (A_{\max} - A_0) / [1 + 10^{(\log IC_{50} - \log X)}] \quad (\text{Eq. 1})$$

where A and A_0 are blank-adjusted protein kinase activity in the presence and absence of inhibitor (at concentration X), respectively. IC₅₀ values were calculated using the nonlinear regression algorithm of GRAPHPAD PRISM (GraphPad Software Inc.).

Crystallization and Data Collection—Purified Cki1Δ298 was concentrated to 12 mg/ml and exchanged into Buffer A (10 mM MOPS, pH 7.0, 0.1 mM EGTA, 0.1% 2-mercaptoethanol, and 100 mM NaCl) using centrifugal filtration. Cki1Δ298:IC261 binary complex was prepared by adding 25 mM inhibitor dissolved in Me₂SO to purified protein to yield a final inhibitor concentration of 500 μM, a final Me₂SO concentration of 2% (v/v), and an inhibitor:protein molar ratio of ≈1.7:1. The addition was made in small aliquots over 30 min at room temperature to overcome the poor aqueous solubility of IC261 and to ensure binary complex formation. Binary complexes were then subjected to crystallization conditions at 16 °C by vapor diffusion as described previously (21), except that final reservoir solution contained 1.5–1.6 M (NH₄)₂SO₄, 5 mM sodium acetate, pH 4.2, and 1% 2-methyl-2,4-pentanediol. These conditions yielded two crystal morphologies: Hexagonal rods (0.28 × 0.1 × 0.1 mm, space group P6₁ with cell dimensions $a = b = 113.5$ Å, $c = 110.4$ Å) that diffracted to 2.8 Å and hexagonal bipyramids (cell dimen-

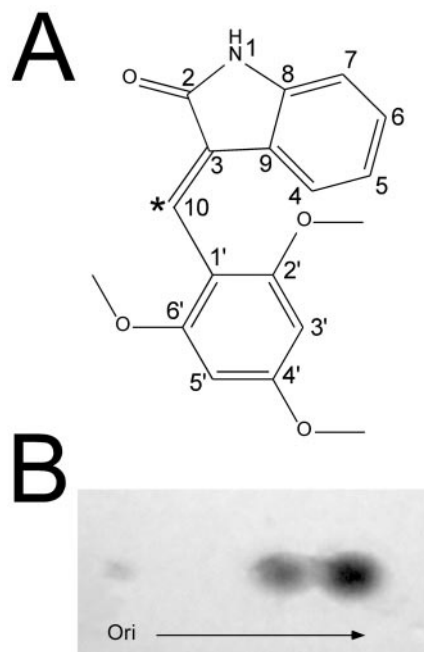


FIG. 1. IC261 structure and nomenclature. A, IC261 is a 3-substituted indolin-2-one derivative with anti-protein kinase inhibitory activity. E and Z geometric isomers of IC261 differ by the position of the trimethoxyphenyl moiety relative to the olefinic bond marked by an asterisk. The E geometric isomer is shown. B, when subjected to thin layer chromatography, IC261 splits into two principal species migrating with R_f values of 0.18 and 0.26. On the basis of NMR analysis, these represent the E and Z geometric isomers of IC261, with the former being the major species. *Ori*, origin, direction of solvent migration.

sions $a = b = 96.4$ Å, $c = 214.4$ Å) that diffracted to 4.0 Å when final Me₂SO concentration was kept <1%. Although these latter crystals grew large, they were consistently mosaic and were not analyzed further.

Binary complex crystals were harvested using a nylon loop, brushed against cryoprotection solution (5 mM sodium acetate, pH 4.2, 2 M (NH₄)₂SO₄, 30% sucrose), and flash frozen in a dry nitrogen stream. All data were collected at -140 °C on a Rigaku R-AXIS IIC image plate system, mounted on a Rigaku RU200-HB rotating anode x-ray generator (Cu Kα) operated at 50 kV and 100 mA. Data were processed with BIOTEX (Rigaku Intl. Corp.) and DENZO/SCALEPACK (31) program packages.

Structure Determination and Refinement—A molecular replacement solution was found using data between 15–3.5 Å, the program AMORE (32) and coordinate set 2CSN as the search model. Initially, data were processed in space group P6₂ with one molecule in the asymmetric unit and cell dimensions $a = b = 113.5$ Å and $c = 55.2$ Å. The rotation function yielded only one peak, and the translation search with that orientation yielded a trial solution with correlation coefficient of 58.5% and R_{cryst} of 38.4%. When further refinement using all data to 2.8 Å failed to improve the R_{cryst} , the diffraction pattern was examined more closely, revealing additional reflections consistent with a double cell along the c -axis. Data were then reprocessed in space group P6₁ with cell dimensions $a = b = 113.5$ Å and $c = 110.4$ Å and reanalyzed in AMORE. Again the rotation function yielded a single peak. During a two-body translation search, two molecules were found in the asymmetric unit shifted by ≈1/2 c (translation vectors of -1.43, 0.54, and 53.8), and related by a 4° rotation about crystal axis b . The correlation coefficient for the correct solution was 66.0% with an R_{cryst} of 36.6%. All successive refinement was done using the program CNS (33), using standard restraints and setting 10% of the data aside to calculate the R_{free} value (34). Rigid body refinement (treating each molecule in the unit cell as a rigid body), was followed by 10 cycles of simulated annealing. After several cycles of refinement, Fourier maps were calculated, and model quality was visually assessed within TURBO-FRODO (35, 36). Solvent molecules were then picked automatically, and the correctness of the assignment was examined by visualizing electron density maps. At this point, Fourier maps (both $2F_o - F_c$ and $F_o - F_c$ maps) showed strong continuous density for the inhibitor. Initial mod-

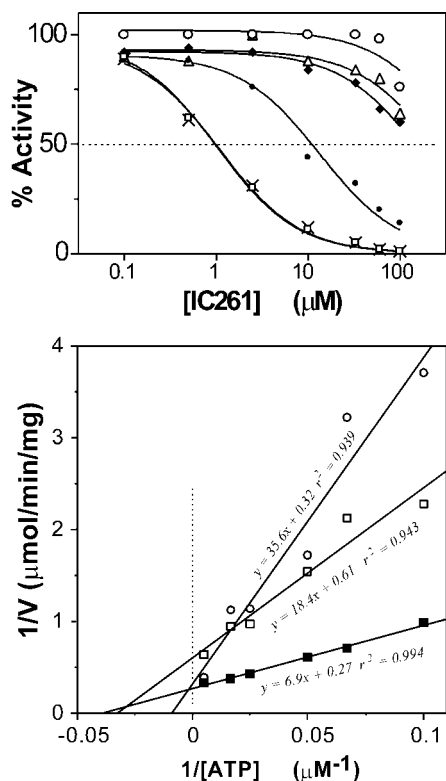


FIG. 2. IC261 is a CK1-selective, ATP-competitive protein kinase inhibitor. *A*, purified samples of protein kinases Cki α (●), Cki δ (□), Cki ϵ (×), p34^{cdc2} (○), p55^{ln} (◆), and PKA (△) were incubated in the presence of protein substrate, 10 μ M ATP, and varying concentrations of IC261 (0.09, 0.5, 2.5, 12.5, 33, 66, and 100 μ M). Plots of the percentage of control activity remaining *versus* IC261 concentration show that IC261 inhibits the closely related Cki δ and Cki ϵ isoforms selectively, with an IC₅₀ (dotted line) of approximately 1 μ M. This value is \approx 10-fold lower than that for Cki α and at least 2 orders of magnitude lower than those estimated for p34^{cdc2}, p55^{ln}, and PKA. *B*, the truncated catalytic domain of Cki1 from *S. pombe* (Cki1 Δ 298) was assayed in the presence of variable concentrations of ATP substrate (10, 15, 20, 40, 60, 80, and 100 μ M) at constant concentration of casein substrate (2 mg/ml) and either 0 (■) or 20 μ M (○) IC261. The inhibition pattern (increase in $K_{m\text{ATP}}$ with little change in V_{max}) confirms that IC261 is a competitive inhibitor of ATP substrate. In contrast IC3608, a representative Class II inhibitor analyzed at 100 μ M (□), showed a noncompetitive inhibition pattern (decrease in V_{max} with little change in $K_{m\text{ATP}}$).

els of IC261 (both E and Z geometric isomers) were generated using TURBO-FRODO, subjected to energy minimization with X-PLOR2D (37), and then manually fit into the density. Topology and parameter files were created for inhibitor, and it was refined along with protein through subsequent cycles of refinement.

Structure Analysis—Nomenclature for amino acid residues, loops, and secondary structure elements was as described in Ref. 23. The final model was characterized using the program PROCHECK (38). Atomic coordinates derived from different models were superpositioned using X-PLOR (39). Main chain atoms (N, C α , C, and O) corresponding to secondary structure elements within the N-terminal (β -strands 3–5 and α -helix A) or the C-terminal (α -helices B–I) domains were used separately to align CK1 models. Domain movements were quantified from superpositioned coordinate sets using HINGEFIND (40).

Analytical Methods—Circular dichroism measurements were performed in the presence (10, 30, and 50 μ M) or absence of IC261 using a Jasco 720 CD spectropolarimeter. Cuvette pathlength and sample concentration were adjusted in diluent (5 mM sodium phosphate, pH 7.0, 50 mM NaClO₄) so that the total optical density was less than 1.0 over the measured spectral range (190–260 nm). Secondary structure content was calculated using the program SELCON (41).

Equilibrium denaturation measurements were performed on Cki1 Δ 298 (0.25 mg/ml) in darkness at room temperature overnight in 0.2 M NaCl, 10 mM HEPES, pH 7.4, and 0–7 M urea in the presence and absence of saturating concentrations of IC261 (100 μ M). Intrinsic Trp/Tyr fluorescence was measured in an SLM 8000c fluorometer over the emission range 300–400 nm upon excitation at 280 nm. Data were

TABLE I
Data collection and refinement statistics

Data collection	
Unit cell dimensions (Å)	$a = b = 113.5; c = 110.4$
Space group	P6 ₁
Data collection temperature (°C)	–140
Reflections	
Maximum resolution (Å)	2.8
measured, unique	98304, 18625
Data completeness (%) ^a	
Overall, outer shell	95.5, 76.4
R_{merge} (%) ^b	10.9
Refinement statistics	
Atoms	
Protein, solvent, sulfate, ligand	4770, 47, 55, 46
R-factor	
R_{cryst} (R_{free}) ^c	22.4 (30.5)
Root mean square deviations from ideals	
bond lengths (Å)	0.008
bond angles (°)	1.463
B-factors (Å ²)	
Main, side, sulfate, solvent, ligand	26.6, 26.5, 42.5, 17.6, 43.6

^a Outer shell, 2.97–2.80 Å.

^b $R_{\text{merge}} = \sum |I_i - \langle I \rangle| / \sum I_i$, where I_i is the intensity of the i th observation and $\langle I \rangle$ is the mean intensity of the reflection, summed over all reflections.

^c R-factor = $\sum \|F_o\| - \|F_c\| / \sum \|F_o\|$, where F_o and F_c are the observed and calculated structure factors, respectively. R_{cryst} was calculated from the 90% of reflections used in refinement, and R_{free} was calculated from the remaining 10%.

analyzed as described in Ref. 42.

NMR spectra of IC261 were recorded using a Bruker DPX 250 MHz NMR spectrometer. Tetramethylsilane was used as an internal standard, and chemical shifts were recorded in parts per million (δ) downfield from this standard.

Geometric isomers of IC261 were resolved by thin layer chromatography on silica gel plates using ethyl acetate/hexane (1:1) as solvent and visualized with ultraviolet light. Statistical errors are reported as standard deviations unless otherwise noted.

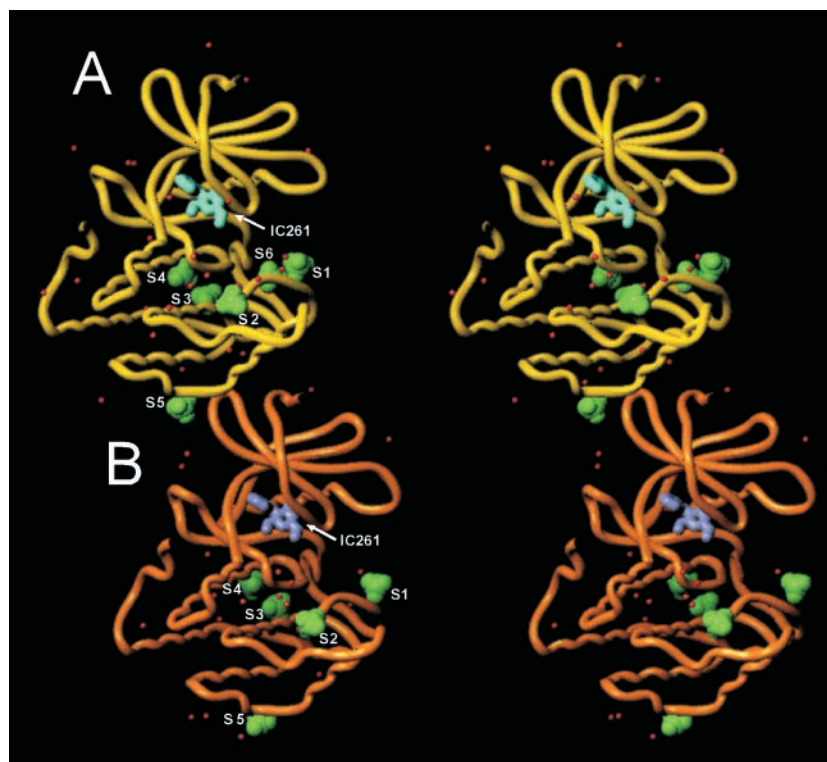
RESULTS

IC261 Is a CK1-selective Protein Kinase Inhibitor—To identify candidate CK1 antagonists, a library of small molecules was screened for inhibitory activity against three mammalian isoforms of CK1 (Cki α , Cki δ , and Cki ϵ) in the presence of low (2 μ M) and high (1 mM) concentrations of nucleotide substrate (ATP). Two broad classes of inhibitor were identified from this screen. Class I consisted of molecules whose inhibitory activity was attenuated at high ATP concentration, suggesting they acted through the nucleotide-binding site. In contrast, Class II molecules inhibited protein kinase activity independently of ATP concentration, consistent with an alternative mechanism of inhibition.

The structure of IC261, a CK1-selective Class I molecule identified by the screen, is shown in Fig. 1A. It is a 3-substituted indolin-2-one derivative. Molecules of this family are commonly prepared by base-catalyzed condensation of aldehydes and oxindole (43, 44) and therefore typically consist of mixtures of E and Z geometric isomers. When subjected to thin layer chromatography, IC261 resolved into two principal species in \sim 2:1 ratio, suggesting that it too was a mixture of geometric isomers (Fig. 1B). NMR analysis revealed a complex pattern consistent with a mixture of two species in a \sim 2:1 ratio (data not shown). The relative signal intensity associated with the presumptive olefinic proton (7.76 ppm for E isomer) was consistent with the E isomer being the predominant geometric isomer in the preparation (data not shown).

To assess relative selectivity, the inhibitory profile of IC261 was extended to include three unrelated protein kinases that were well characterized structurally and enzymologically: PKA, p34^{cdc2}, and *src* homolog p55^{ln} (Fig. 2, top). When as-

FIG. 3. Overall structure of the IC261-Cki1 Δ 298 binary complex. The complex crystallized in space group P6₁, with the asymmetric unit containing two protein molecules (labeled A and B) arranged head-to-tail. Each polypeptide chain folded into an N-terminal domain containing five antiparallel β -strands (β 1–5) and one α -helix (α A) and into a C-terminal domain containing four antiparallel β -strands (β 6–9) and eight α -helices (α B-1) as described previously (22, 23). The final model also contained 11 sulfate ions (S1–S6, shown in green), 47 water molecules (shown in red), and two IC261 molecules distributed between the protein molecules A and B.



sayed at 10 μ M ATP, IC261 was most potent against Cki δ ($IC_{50} = 1.0 \pm 0.3 \mu$ M) and Cki ϵ ($IC_{50} = 1.0 \pm 0.4 \mu$ M), followed by Cki α_1 ($IC_{50} = 16 \pm 5 \mu$ M), followed by PKA, p34^{cdc2}, and p55^{lyn} (IC_{50} s > 100 μ M). Together these data suggest that one or both geometric isomers of IC261 selectively inhibit CK1 isoforms compared with unrelated protein kinases represented in the test group. Moreover, the results obtained from this pilot screen suggest that it is possible to isolate inhibitors with an order of magnitude selectivity for individual CK1 isoforms.

IC261 Is a Competitive Inhibitor of Nucleotide Substrate—As a Class I inhibitor, IC261 was predicted to inhibit protein kinases by competing with the binding of ATP substrate. To test this hypothesis, the ability of IC261 to inhibit Cki1 Δ 298, a truncation mutant of *S. pombe* Cki1 (21), was characterized by steady state kinetics. This particular CK1 isoform was chosen for analysis because it consists of only the catalytic domain of CK1 and because its structure is known at high resolution in complex with ATP (22) and at medium resolution in complex with an ATP-competitive isoquinoline sulfonamide inhibitor (23). In the absence of IC261, Cki1 Δ 298 returned a K_m for ATP of $25.6 \pm 0.2 \mu$ M and a V_{max} of $3.7 \pm 0.2 \mu$ mol/min/mg (Fig. 2, bottom). In the presence of IC261, the V_{max} changed little ($3.1 \pm 0.2 \mu$ mol/min/mg), whereas the apparent K_m ATP increased to $111 \pm 0.2 \mu$ M. This pattern is identical to those exhibited by ATP-competitive agents such as the isoquinoline sulfonamide CKI7 (18, 23). In contrast, IC3608, a representative Class II inhibitor, lowered V_{max} (1.6 ± 0.2 mg/min/mg) but had little effect on the K_m ATP ($30.2 \pm 0.3 \mu$ M). These results confirm that IC261 inhibition is competitive with respect to ATP.

To determine whether IC261 binding was accompanied by changes in CK1 secondary structure, circular dichroism measurements were performed on Cki1 Δ 298 in the presence and absence of nucleotide or IC261 ligand. The resultant spectra were virtually identical in all cases, suggesting that binding of IC261 to CK1 was not accompanied by measurable changes in Cki1 Δ 298 secondary structure (data not shown). Consistent with this observation, the sensitivity of Cki1 Δ 298 to urea de-

naturation was unchanged in the presence or absence of IC261. Half-maximal denaturation was observed in ≈ 3.3 M urea, yielding an extrapolated free energy of folding of 11.2 ± 0.79 kcal/mol (data not shown). Together these data suggest that one or both geometric isomers of IC261 bound in the ATP-binding cleft of Cki1 Δ 298 and that binding did not induce measurable changes in protein secondary structure.

Crystallization of IC261 in Complex with Cki1 Δ 298—To clarify the mechanism of IC261 selectivity, it was crystallized in complex with Cki1 Δ from solutions containing ammonium sulfate at acidic pH. Although the binary complex of Cki1 Δ ·MgATP forms highly ordered trigonal crystals under these conditions (21), no crystals of this space group were formed from Cki1 Δ 298·IC261 binary complex. Instead, hexagonal rods of space group P6₁ that diffracted to 2.8 Å resolution were consistently obtained. Complete native data sets were collected from individual crystals, and the structure was solved by molecular replacement. Data collection and refinement statistics are presented in Table I. The final model contained two Cki1 Δ 298 molecules in the asymmetric unit (termed molecules A and B) arranged head-to-tail (Fig. 3). As in our previous CK1 crystal structures (22, 23), residues 1–5 and 222–226 were disordered, and Val¹⁰ was modeled with disallowed backbone torsion angles in both molecules A and B. All remaining amino acid residues had appropriate backbone torsion angles, with 94% lying in the most favorable, and additionally allowed regions of the Ramachandran plot (calculated for 514 non-Gly and non-Pro residues present in both molecules of the asymmetric unit).

The protein molecules were accompanied by 47 well ordered water molecules and 11 sulfate ions (Fig. 3), four of which occupied the S1 and S2 sites described previously (22). In molecule A, the S1 site, a pocket ringed by Arg¹³⁰, Lys¹⁵⁹, Lys¹⁷⁵, Lys¹⁷⁶, and Asp¹⁹⁴, was modeled with an additional sulfate (S6), whereas in molecule B it was modeled with a single sulfate ion in association with two water molecules. The six remaining sulfates occupied three sites in each molecule. The S-3/S-4 sites were located within a pocket formed by the

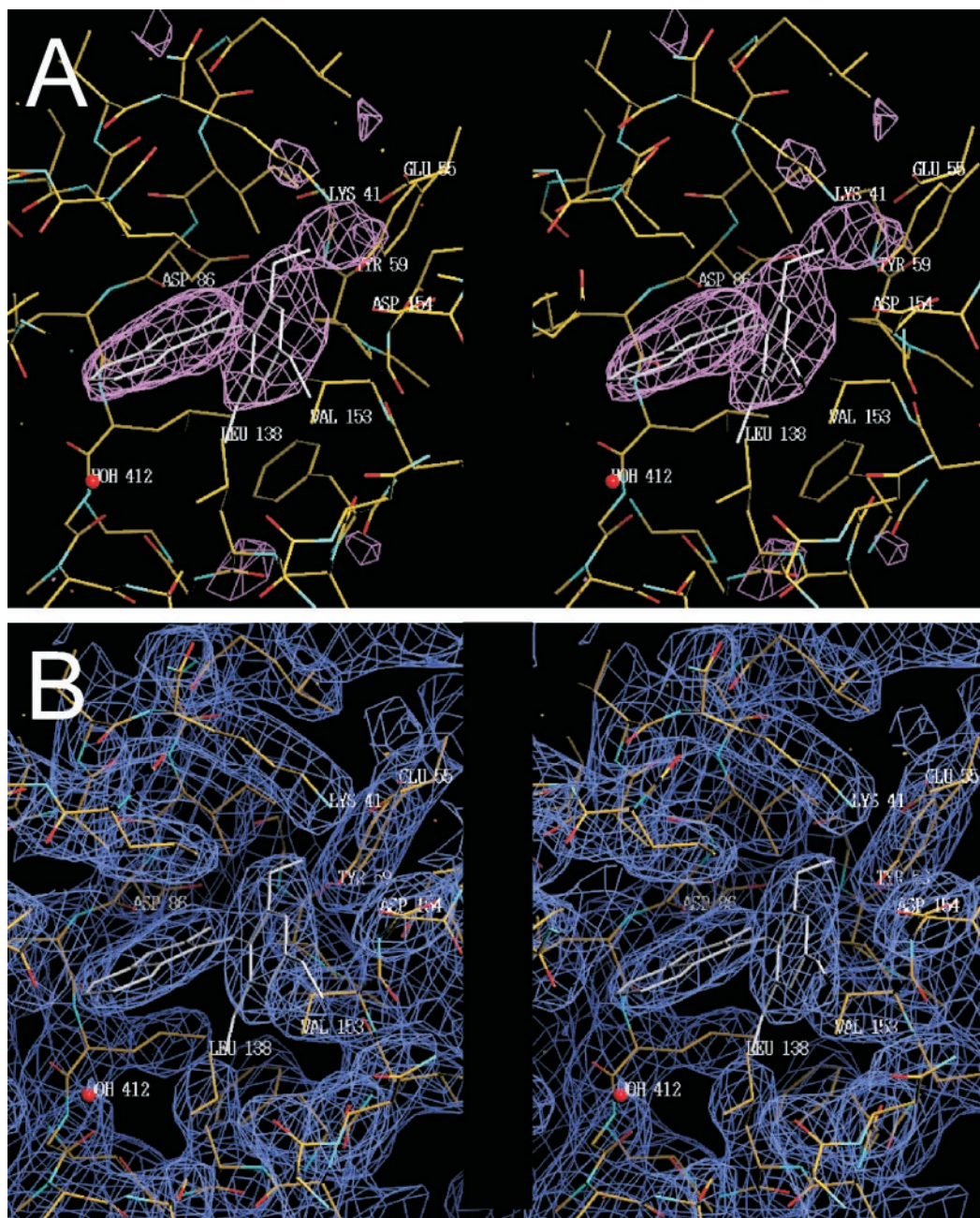


FIG. 4. IC261 binds Cki1 Δ 298 in the nucleotide substrate cleft. IC261 electron density was displayed in stereo using TURBO-FRODO. A, positive $F_o - F_c$ difference density in the ATP-binding site of Cki1 Δ 298 contoured at 2.5σ . The map was calculated after refinement of protein atoms but before placement of any inhibitor atoms (the IC261 model is displayed for reference only). The planar density corresponding to the oxindole and trimethoxyphenyl rings was best fit by IC261 in the E conformation. B, $2F_o - F_c$ map of the fully refined binary complex computed at 2.8 Å resolution and contoured at 1σ . Carbon atoms are colored yellow, oxygen atoms are red, and nitrogen atoms are blue.

side chains of Arg¹⁶², Lys¹⁶⁷, His¹⁶⁹, and Arg¹⁹⁷ and correspond to a tungstate-binding site identified previously in the mammalian Cki δ model (1CKJ; residue 401). The remaining sulfates occupied a novel site (S5) formed at the junction of the two protein molecules by the side chains of Arg²⁴³ and His²⁵⁸ and the main chain nitrogen of Asn³⁵.

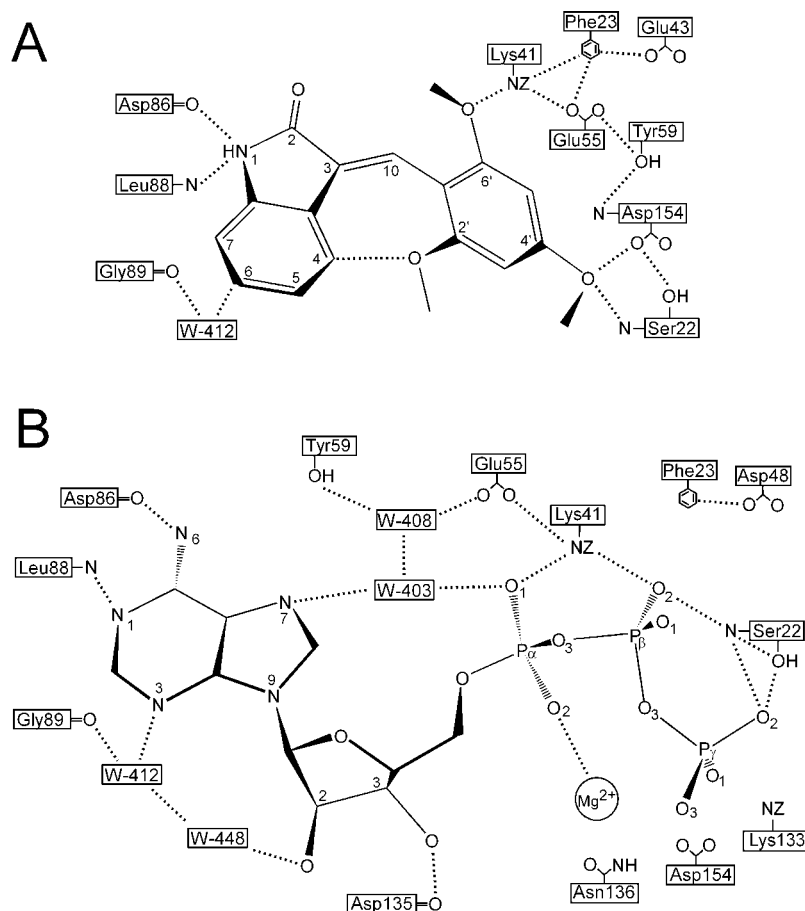
CK1 Inhibition Is Specific for the E Geometric Isomer of IC261—Each protein molecule contained clear electron density for the two aromatic rings of IC261 and for the olefinic linker connecting them, leading to unambiguous placement within the model (Fig. 4A). At 2.8 Å resolution, the bound conformation of IC261 refined as the E geometric isomer with near ideal bond lengths and angles. The olefinic bond was within $1.9 \pm 0.8^\circ$ of planarity, whereas the dihedral angle between the two aromatic rings averaged $56.0 \pm 2.1^\circ$ (in both molecules of the

asymmetric unit), which was within 6.0° of the angle predicted by energy minimization. This conformation was stabilized by van der Waals' contact (bond length = 3.1 Å) between the edge of the aromatic oxindole nucleus (C-4) and methoxy O-2'.

Electron density for IC261 was contained entirely within the nucleotide-binding cleft, formed by the junction between the α -helix-rich C-terminal domain and the smaller, β -sheet-containing N-terminal domain. The oxindole nucleus occupied the pocket previously identified as P-1 (23), which normally hosts the adenine ring of ATP (in 1CSN) and the isoquinoline nucleus of inhibitor CKI7 (in 2CSN). It was oriented so that its carbonyl group extended toward the interior of the binding cleft to within 4.5 Å of the phenol moiety of Tyr⁵⁹ (Fig. 4B). When all three structures were superpositioned, the adenine and isoquinoline nuclei were nearly coplanar, whereas the oxindole

FIG. 5. Schematic representation of hydrogen and electrostatic interactions between Cki1Δ298 and ligands.

The distances of all hydrogen bonds (dotted lines) = 3.4 Å in length are shown (for clarity, hydrophobic interactions are not illustrated). **A**, binding of the E geometric isomer of IC261 to Cki1Δ298 stabilizes a network of hydrogen bonds among residues lining the nucleotide substrate-binding pocket. In molecule A, the network extends to include hydrogen bonds between OD2 of Asp¹³¹ and OG of Ser²² and ND2 of Asn¹³⁶. IC261 interacts directly with the network through hydrogen bonds between its trimethoxyphenyl moiety and the side chains of Lys⁴¹, Ser²², and Asp¹⁵⁴. In contrast, the oxindole nucleus binds primarily through hydrophobic interactions with the side chains of Ile¹⁸, Ile²⁶, Ala³⁹, Leu¹²⁸, and Val¹⁵³. In molecule A, water 412 bridges the carbonyl of Gly⁸⁹ with the edge of the oxindole ring. This interaction was not observed in molecule B. Instead, N-1 of the oxindole ring made hydrogen bonds to the main chain nitrogen of Leu⁸⁸ and the carbonyl group of Asp⁸⁶. **B**, in the Cki1Δ298·MgATP complex (22), binding is mediated by many of the same residues that contact IC261. But instead of an extended network of interactions, more direct (or water-mediated) hydrogen bonds exist between ligand and protein.



nucleus differed by $\approx 15^\circ$. Moreover, the hydrophobic contacts made between CK1 and the oxindole nucleus were nearly identical to those described previously for the adenine nucleus (22), and the ring nitrogen of oxindole (N-1) was within 1 Å of adenine N-1 and isoquinoline N-2. Despite these similarities, closer inspection revealed that the oxindole nucleus did not fill the P-1 site as fully as did adenine and that different modes of binding could be distinguished in the two molecules of the asymmetric unit (Fig. 5A). In molecule A, the electropositive edge of aromatic C-6 was bonded to main chain carbonyl of Gly⁸⁹ through a water molecule (water 412). A similar interaction was observed between N-3 of ATP, water 412, and Gly⁸⁹ in model 1CSN (22). In this position, however, N-1 of the oxindole nucleus was outside hydrogen bonding distance of the main chain nitrogen of Leu⁸⁸. In molecule B, no water-mediated bridge to Gly⁸⁹ was observed, but N-1 was within hydrogen bonding distance (3.4 Å) of both the main chain nitrogen of Leu⁸⁸ and the carbonyl of Asp⁸⁶. These data suggest that the oxindole nucleus binds the P-1 site of CK1 through a subset of the same pharmacophores that bind and position the adenine and isoquinoline nuclei of ATP and CKI7 (Fig. 5B).

An olefinic bridge connects the trimethoxy phenyl moiety of IC261 to the oxindole nucleus. This moiety was located at the rear of the ATP-binding pocket in van der Waals' contact with Val¹⁵³. The trimethoxy phenyl moiety itself extended into that portion of the nucleotide-binding cleft previously identified as the P3 region, which normally binds the phosphate groups of ATP (22, 23). There, the O-4' methoxy group of IC261 occupied a position nearly identical to the O-2 atom of ATP α -phosphate in model 1CSN. In contrast to ATP, however, the aromatic ring of IC261 was held in position by two hydrophobic surfaces formed by the glycine-rich loop (in particular the side chain of Ile²⁶) on one side and by Val¹⁵³ and the aliphatic side chain of

Asp¹⁵⁴ on the other. In addition, hydrogen bonds formed between the methoxy groups of the ring and CK1 (Fig. 5A). As mentioned above, methoxy O-2' interacts with the electropositive edge of the oxindole nucleus. Methoxy O-4' was within hydrogen bonding distance of both atom OD2 of catalytic residue Asp¹⁵⁴ and the main chain nitrogen of Ser²², whereas methoxy O-6' made contact with the NZ atom of the catalytic residue Lys⁴¹.

Although contacts between IC261 and CK1 were limited, binding was accompanied by formation of an extended network of hydrogen and electrostatic bonds among CK1 residues Ser²², Phe²³, Lys⁴¹, Glu⁴³, Glu⁵⁵, Tyr⁵⁹, and Asp¹⁵⁴ (Fig. 5A). In molecule B, this network expanded to include side chains of Asp¹³¹ and Asn¹³⁶. These data are consistent with the binding energy of IC261 being used to stabilize a network of interactions that span both N- and C-terminal domains of CK1.

IC261 Is a Conformation-selective Inhibitor—Although IC261 was bound completely within the ATP-binding cleft, it proved consistently impossible to seed crystals in the trigonal space group corresponding to the “closed,” ATP-bound form of Cki1Δ298. This observation, along with the novel hydrogen bonding network described above, suggested that IC261 binding was accompanied by changes in Cki1Δ298 conformation. To test this hypothesis, coordinates for molecules A and B of the Cki1Δ298·IC261 binary complex were superpositioned on the established coordinates of Cki1Δ298·MgATP (1CSN). Superposition of C-terminal domains (root mean square deviation of C_α positions was 0.40 and 0.48 for molecules A and B, respectively) revealed a significant movement of the N-terminal domain (residues 6–89) relative to the C-terminal domain (residues 90–298) in the two models (Fig. 6, top). Within the C-terminal domain, all differences in C_α positions (ΔC_α) in excess of 1 Å were localized to loops L-BC, L-78, L-9D, L-EF, and the random

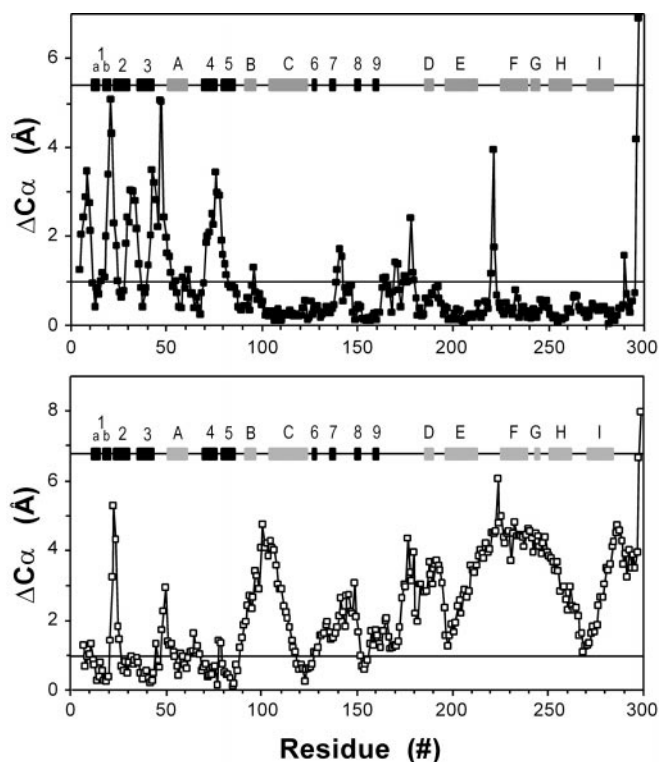


FIG. 6. Conformational changes accompany Cki1 Δ 298 binding of IC261. Distances between equivalent α -carbon atom positions in Cki1 Δ 298 when complexed with MgATP versus inhibitor IC261 were calculated after superposition of C-terminal domains (top) and superposition of N-terminal domains (bottom) and plotted as a function of residue number. Boxes delineate secondary structure elements (black, β -strands 1–9; gray, α -helices A–I). The source of $\Delta C_{\alpha} > 1 \text{ \AA}$ are described in the text.

coil C-terminal segment. Although changes in the latter two segments were large, they appeared unrelated to ligand binding because L-EF is disordered in all CK1 crystal structures to date and the C-terminal random coil was displaced by crystal contacts. Thus movement of the remaining loops appeared to derive from ligand binding. Superposition of N-terminal domains (root mean square deviation of C_{α} positions was 0.62 and 0.74 for molecules A and B, respectively) showed that ΔC_{α} values of $>1 \text{ \AA}$ were limited to loops L-12 (*i.e.* the glycine-rich loop), L-3A, L-A4, L-45, and the random coil N-terminal segment (Fig. 6, bottom). Differences in the N terminus and L-45 derived from crystal packing constraints, whereas movement of the other segments resulted from ligand binding. Together these data are consistent with the IC261 binding being accompanied by a rigid body rotation of the N-terminal domain relative to the C-terminal domain and by ancillary changes in six surface loops.

To quantify the rotation, the C-terminal domains of Cki1 Δ 298-IC261 and Cki1 Δ 298-MgATP (1CSN) were superpositioned, and the relative movement of the N-terminal domain was analyzed with the program HINGEFIND (39). Although only 56% identical in amino acid sequence to *S. pombe* Cki1 Δ 298, mammalian CK1 (1CKJ) was included in the analysis so as to provide a model of CK1 in a non-liganded conformation. Analysis of the pair 1CSN/1CKJ revealed that MgATP substrate binding is associated with a 12° rigid body rotation around an axis lying perpendicular to the ATP-binding pocket (Fig. 7). In contrast, the pair 1CSN/Cki1 Δ 298-IC261 were related by a rotation angle of only $7.0 \pm 1.6^{\circ}$ (mean \pm range of molecules A and B) along an axis similar but not identical to that found for 1CSN/1CKJ. These data show that the IC261-bound conformation of CK1 is distinct and lies approxi-

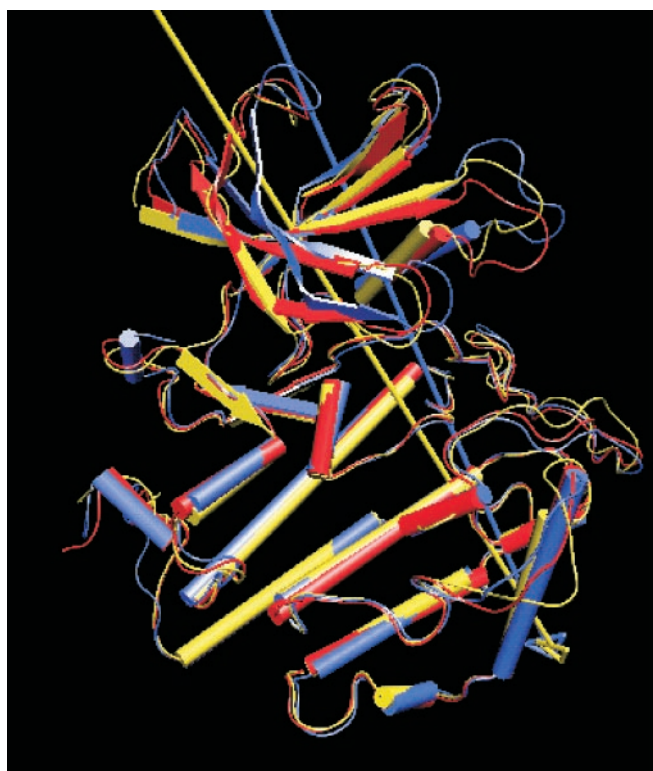


FIG. 7. IC261 binding is accompanied by a rigid body rotation of domains. C-terminal domains of CK1 bound with ATP substrate (1CSN; red), with IC261 (yellow), and without ligand (1CKJ; blue) were superpositioned as described under "Experimental Procedures." The rotation axes required to align the N-terminal β -sheet of 1CKJ (blue) and IC261 binary complex (yellow) with that of 1CSN were then calculated using HINGEFIND as 12° and $7.0 \pm 1.6^{\circ}$ (means \pm range of molecules A and B), respectively. The alignment of 1CSN and Cki1 Δ 298-IC261 was accompanied by a projection angle of $9.8 \pm 1.1^{\circ}$ (mean \pm range of molecules A and B), consistent with a rigid body rotation (39).

mately midway between its nonliganded and ATP-bound conformations.

In light of this rigid body rotation, the changes in conformation of the six surface loops identified above were reassessed. On closer inspection, most changes were related to the rigid body rotation as was found by comparing nonliganded and ATP-bound forms of CK1 (data not shown). In the C-terminal domain, L-78 moved because the side chain of Arg¹⁴¹ hydrogen bonds with Asn³⁷, a residue that rotates as part of the N-terminal domain. L-BC appeared to move relative to the C-terminal domain because Asp⁹⁴ no longer bound the ribose moiety of ATP through water, whereas residues 179–180 of L-9D moved as a result of Lys¹³³ no longer making contact with the γ -phosphate of ATP. In the N-terminal domain, L-A4 appeared to move relative to the N-terminal domain because it stayed in contact with the C-terminal domain. In contrast, movement of both the glycine-rich loop and L-3A were related to each other but distinct from the rigid body rotation. Residues of the glycine-rich loop made direct contact with inhibitor, stabilizing the loop so that Phe²³ bonded to the side chain of Glu⁴³ instead of Asp⁴⁸, as it does in the ATP-bound structure. Because L-3A makes direct contact with the glycine-rich loop, different G-loop conformations lead to different conformations of L-3A in the two structures. These data are consistent with the E geometric isomer of IC261 stabilizing a unique conformation of CK1 so that an extended network of hydrogen and electrostatic bonds spanning the N- and C-terminal domains of the enzyme can form and render it inactive.

DISCUSSION

IC261 is a new CK1-selective inhibitor with up to 1 order of magnitude greater affinity for certain CK1 isoforms than the isoquinoline sulfonamide inhibitor, CKI7. It is uncharged at physiological pH and can diffuse across cell membranes. Indeed, IC261 has been shown to inhibit Cki δ in intact murine SV3T3 cells (46). The selectivity and affinity of IC261 for CK1 isoforms stems from an induced fit mechanism. It binds a subset of the substrate-binding pharmacophores lying in the nucleotide-binding cleft resulting in stabilization of CK1 in a conformation that is midway between the unliganded and nucleotide-bound forms of the enzyme. This conformation is further stabilized by additional movement of the glycine-rich loop, which makes contact with IC261 and simultaneously participates in a novel hydrogen and electrostatic bond network involving aromatic, charged, and polar amino acid residues spanning both domains. The stability of this network of delocalized interactions decreases the dissociation rate of the inhibitor, resulting in a measurable decrease in apparent IC₅₀ for members of the CK1 family relative to other protein kinases. Although Cki1 Δ 298 was crystallized from solutions containing both E and Z geometric isomers of IC261, the results presented here suggest that the E isomer is the energetically favored inhibitory form.

In contrast, it was shown previously that inhibition of receptor tyrosine kinases, such as FGFR, could be achieved with 3-substituted indolin-2-one derivatives in the Z conformation, such as SU4984 and SU5402 (43). Crystal structures of these ligands in complex with FGFR kinase revealed, however, that binding was accompanied by significant strain in ligand conformation. For example, both SU4984 (2.4 Å resolution) and SU5402 (2.5 Å resolution) were modeled with the olefinic bond bridging the oxindole and R group possessing substantial single bond character (the olefinic bonds in these models averaged 1.50 ± 0.05 Å in length, which is nearly 0.2 Å longer than ideal double bond length). Moreover, these bonds were distorted from planarity an average of $26.8 \pm 2.0^\circ$ and $12.7 \pm 2.1^\circ$ in the models of SU4984 and SU5402, respectively, corresponding to an energy penalty of up to 2.5 kcal/mol. Binding of SU5402 also led to a significant reduction in β -sheet conformation of amino acid residues of the glycine-rich loop. In contrast, the structure of Cki1 Δ 298-IC261 complex had near ideal bond lengths and angles for IC261 without modification of protein secondary structure. Distortion of both ligand and polypeptide in FGFR kinase complexes may have resulted from soaking existing crystals of apoenzyme in ligand rather than resorting to *de novo* crystal growth of inhibitor-enzyme binary complex as was done here. Indeed, we were unable to prepare IC261-Cki1 Δ 298 crystals in trigonal morphology (*i.e.* the fully closed conformation of CK1) by microseeding, suggesting it would have been difficult to obtain the IC261-bound conformation by merely soaking existing crystals in IC261.

Structure activity relationship data prove that receptor tyrosine kinases can accommodate E as well as Z geometric isomers of 3-substituted indolin-2-one depending on the properties of substituent groups (44). Comparison of the SU4984/5402 and IC261 crystal structures reveals that this can be accomplished by flipping of the indolin-2-one nucleus so that the carbonyl moiety at the 2 position points either toward the nucleotide-binding pocket, as the E isomer of IC261 does in complex with CK1, or outward toward solvent, as do the Z geometric isomers of SU4984/5402 in complex with FGFR (Fig. 8). In either conformation, the indolin-2-one nucleus is within 15° of being coplanar with the adenine ring of ATP substrate and retains the ability to hydrogen bond main chain atoms in the hinge region (23) through its N-1 nitrogen. We showed

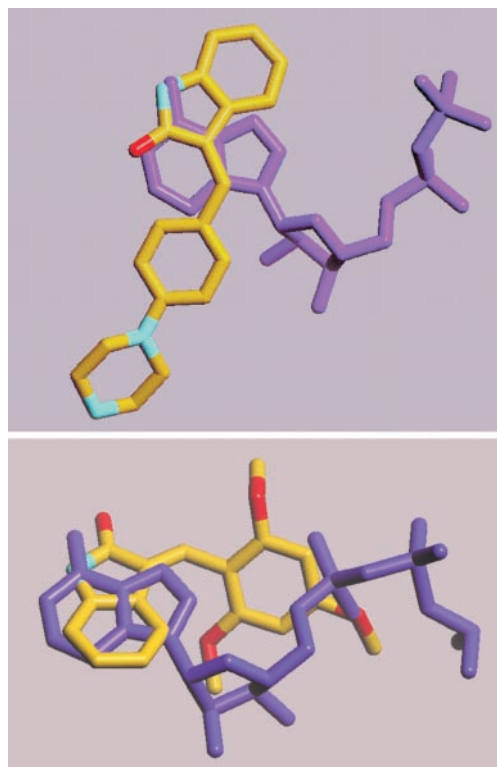


FIG. 8. Protein kinases bind both E and Z geometric isomers of indolin-2-one derivatives. A, model of the E geometric isomer of IC261 (yellow) derived from the IC261-Cki1 Δ 298 binary structure. The relative location of ATP (purple) after superpositioning of IC261-Cki1 Δ 298 binary complex and 1CSN models is shown for orientation. B, model of Z geometric isomer of SU4984 (yellow) in complex with FGFR kinase (1AGW). The relative location of ATP analog AMP-PCP (purple) after superpositioning of SU4984-FGFR and AMP-PCP-FGFR kinase structures (25) is shown for orientation. Although the oxindole ring occupies the adenine-binding pocket in both models, the rings are flipped relative to one another.

previously that flipping of the ring occupying the P-1 site contributes to the selectivity of isoquinoline sulfonamides for individual protein kinases (23, 47).

Pharmacological modulation of protein conformation has been shown to be an effective mechanism for controlling protein activity (*e.g.* 48). Because all protein kinases examined to date are capable of undergoing the conformational changes described here, conformational inhibition may emerge as a general strategy for controlling protein kinase activity. Although the N- and C-terminal lobes of most protein kinases are thought to move relative to each other along a defined pathway (49), both the precise location of axes of rotation and the extent of rotation differs among protein kinases (reviewed by Ref. 50). For example, the rotation axis of CK1 lies perpendicular to the nucleotide-binding site (51), whereas that for PKA lies parallel to helix E located in the C-terminal domain (52). In addition to differences in axis location and degree of rotation, conformations that are intermediate between liganded and nonliganded can be exploited by inhibitors as shown here for CK1 and as shown previously for PKA (53, 54).

The mechanism of inhibition found here shows promise for developing CK1-isoform selective antagonists. Although such reagents would be useful for examining the role of CK1 isoforms in cell regulation, the practicality of ATP-competitive inhibitors for therapeutics has been questioned owing to the high intracellular concentrations of inhibitor needed to overcome physiological levels of ATP (55). Therefore, the non-ATP competitive CK1 antagonists (Class II) identified in our initial screens are also of great interest. Elucidating the mechanism of

action of the latter reagents may yield valuable information applicable to the protein kinase family as a whole.

Acknowledgments—We thank Prof. W. Anderson, Prof. L. Lorand, and Dr. B. Shoichet (all of Northwestern University Medical School, Chicago, IL) for generous access to their x-ray equipment, fluorometer, and circular dichroism spectropolarimeter, respectively. Dr. M. Cicirelli and his HTS group (ICOS Corp., Bothell, WA) are gratefully acknowledged for assistance with chemical screening. X-ray diffraction data collection was supported in part by the Macromolecular Crystallography and Biochemical Computation Resource of Northwestern University Medical School.

REFERENCES

- Gross, S. D., and Anderson, R. A. (1998) *Cell. Signal.* **10**, 699–711
- Vancura, A., Sessler, A., Leichus, B., and Kuret, J. (1994) *J. Biol. Chem.* **269**, 19271–19278
- Wang, P.-C., Vancura, A., Desai, A., Carmel, G., and Kuret, J. (1994) *J. Biol. Chem.* **269**, 12014–12023
- Gietzen, K. F., and Virshup, D. M. (1999) *J. Biol. Chem.* **274**, 32063–32070
- Hoekstra, M. F., Liskay, R. M., Ou, A. C., Demaggio, A. J., Burbee, D. G., and Heffron, F. (1991) *Science* **253**, 1031–1034
- Dhillon, N., and Hoekstra, M. F. (1994) *EMBO J.* **13**, 2777–2787
- Robinson, L. C., Menold, M. M., Garrett, S., and Culbertson, M. R. (1993) *Mol. Cell. Biol.* **13**, 2870–2881
- Kloss, B., Price, J. L., Saez, L., Blau, J., Rothenfluh, A., Wesley, C. S., and Young, M. W. (1998) *Cell* **84**, 97–107
- Peters, J. M., McKay, R. M., McKay, J. P., and Graff, J. M. (1999) *Nature* **401**, 345–350
- Sakanaka, C., Leong, P., Xu, L., Harrison, S. D., and Williams, L. T. (1999) *Proc. Natl. Acad. Sci.* **96**, 12548–12552
- Decottignies, A., Owsianik, G., and Ghislain, M. (1999) *J. Biol. Chem.* **274**, 37139–37146
- Wang, X., Hoekstra, M. F., Demaggio, A. J., Dhillon, N., Vancura, A., Kuret, J., Johnston, G. C., and Singer, R. A. (1996) *Mol. Cell. Biol.* **16**, 5375–5385
- Panek, H. R., Stepp, J. D., Engle, H. M., Marks, K. M., Tan, P. K., Lemmon, S. K., and Robinson, L. C. (1996) *EMBO J.* **16**, 4194–4204
- Murakami, A., Kimura, K., and Nakano, A. (1998) *J. Biol. Chem.* **274**, 3804–3810
- Kuret, J., Johnson, G. S., Cha, D., Christenson, E. R., Demaggio, A. J., and Hoekstra, M. F. (1997) *J. Neurochem.* **69**, 2506–2515
- Ghoshal, N., Smiley, J. F., Demaggio, A. J., Hoekstra, M. F., Cochran, E. J., Binder, L. I., and Kuret, J. (1999) *Am. J. Pathol.* **155**, 1163–1172
- Schwab, C., Demaggio, A. J., Ghoshal, N., Binder, L. I., Kuret, J., and McGeer, P. L. (2000) *Neurobiol. Aging* **17**, in press
- Chijiwa, T., Hagiwara, M., and Hidaka, H. (1989) *J. Biol. Chem.* **264**, 4924–4927
- Hidaka, H., Hagiwara, M., and Chijiwa, T. (1991) *Neurochem. Res.* **15**, 431–434
- Meggio, F., Shugar, D., and Pinna, L. A. (1990) *Eur. J. Biochem.* **187**, 89–94
- Carmel, G., Leichus, B., Cheng, X., Patterson, S. D., Mirza, U., Chait, B. T., and Kuret, J. (1994) *J. Biol. Chem.* **269**, 7304–7309
- Xu, R., Carmel, G., Sweet, R. M., Kuret, J., and Cheng, X. (1995) *EMBO J.* **14**, 1015–1023
- Xu, R.-M., Carmel, G., Kuret, J., and Cheng, X. D. (1996) *Proc. Natl. Acad. Sci. U. S. A.* **93**, 6308–6313
- Kaczmarek, L. K., Jennings, K. R., Strumwasser, F., Nairn, A. C., Walter, U., Wilson, F. D., and Greengard, P. (1980) *Proc. Natl. Acad. Sci. U. S. A.* **77**, 7487–7491
- Mohammadi, M., Schlessinger, J., and Hubbard, S. R. (1996) *Cell* **86**, 577–587
- Hoekstra, M., Dhillon, N., Carmel, G., Demaggio, A. J., Lindberg, R. A., Hunter, T., and Kuret, J. (1994) *Mol. Biol. Cell* **5**, 877–886
- Casnellie, J. E. (1991) *Methods Enzymol.* **200**, 115–120
- Kemp, B. E., Graves, D. J., Benjamini, E., and Krebs, E. G. (1977) *J. Biol. Chem.* **252**, 4888–4894
- Beaudette, K. N., Lew, J., and Wang, J. H. (1993) *J. Biol. Chem.* **268**, 20825–20830
- Cheng, H. C., Nishio, H., Hatase, O., Ralph, S., and Wang, J. H. (1992) *J. Biol. Chem.* **267**, 9248–9256
- Otwinowski, Z., and Minor, W. (1997) *Methods Enzymol.* **276**, 307–326
- Navaza, J. (1994) *Acta Crystallogr. Sect. A* **50**, 157–163
- Brünger, A. T., Adams, P. D., Clore, G. M., DeLano, W. L., Gros, P., Grosse-Kunstleve, R. W., Jiang, J. S., Kuszewski, J., Nilges, M., Pannu, N. S., Read, R. J., Rice, L. M., Simonson, T., and Warren, G. L. (1998) *Acta Crystallogr. D Biol. Crystallogr.* **54**, 905–921
- Brünger, A. T. (1992a) *Nature* **355**, 472–475
- Jones, T. A. (1985) *Methods Enzymol.* **115**, 157–171
- Cambillau, C., and Rossel, A. (1997) *Turbo Fordo*, Version OpenGL. 1, Université Aix-Marseille II, Marseille, France
- Kleywegt, G. J., and Jones, T. A. (1997) *Methods Enzymol.* **277**, 208–230
- Laskowski, R. A., MacArthur, M. W., Moss, D. S., and Thornton, J. M. (1993) *J. Appl. Crystallogr.* **26**, 283–291
- Brünger, A. T. (1992) *X-PLOR*, version 3.1, Yale University Press, New Haven, CT
- Wriggers, W., and Schulten, K. (1997) *Proteins Struct. Funct. Genet.* **29**, 1–14
- Sreerama, N., and Woody, R. W. (1993) *Anal. Biochem.* **209**, 32–44
- Santoro, M. M., and Bolen, D. W. (1988) *Biochemistry* **27**, 8063–8068
- Mohammadi, M., McMahon, G., Sun, L., Tang, C., Hirth, P., Yeh, B. K., Hubbard, S. R., and Schlessinger, J. (1997) *Science* **276**, 955–960
- Sun, L., Tran, N., Tang, F., App, H., Hirth, P., McMahon, G., and Tang, C. (1998) *J. Med. Chem.* **41**, 2588–2603
- Thomas, K. A., Smith, G. M., Thomas, T. B., and Feldman, R. J. (1982) *Proc. Natl. Acad. Sci. U. S. A.* **79**, 4843–4847
- Knippschild, U., Milne, D. M., Campbell, L. E., Demaggio, A. J., Christenson, E., Hoekstra, M. F., and Meek, D. W. (1997) *Oncogene* **15**, 1727–1736
- Engh, R. A., Girod, A., Kinzel, V., Huber, R., and Bossemeyer, D. (1996) *J. Biol. Chem.* **271**, 26157–26164
- Foster, B. A., Coffey, H. A., Morin, M. J., and Rastinejad, F. (1999) *Science* **286**, 2507–2510
- Williams, J. C., Weijland, A., Gonfloni, S., Thompson, A., Courneige, S. A., Superti-Furga, G., and Wierenga, R. K. (1997) *J. Mol. Biol.* **274**, 757–775
- Johnson, L. N., Lowe, E. D., Noble, M. E. M., and Owen, D. J. (1998) *FEBS Lett.* **430**, 1–11
- Longenecker, K. L., Roach, P. J., and Hurley, T. D. (1996) *J. Mol. Biol.* **257**, 618–631
- Zheng, J., Knighton, D. R., Xuong, N.-H., Taylor, S. S., Sowadski, J. M., and Ten Eyck, L. F. (1993) *Protein Sci.* **2**, 1559–1573
- Naryana, N., Cox, S., Nguyen-huu, X., Ten Eyck, L. F., and Taylor, S. S. (1997) *Structure* **5**, 921–935
- Prade, L., Engh, R. A., Girod, A., Kinzel, V., Huber, R., and Bossemeyer, D. (1997) *Structure* **5**, 1627–1637
- Penn, R. B., Parent, J.-L., Pronin, A. N., Panettieri, R. A., and Benovic, J. L. (1999) *J. Pharmacol. Exp. Ther.* **288**, 428–437